

Tribological Behavior of Thermal Spray and Fusing Ni-Based Alloy Coatings with Rare Earth Cerium Under Reciprocating Sliding

Bunv Liang¹ · Zhenyu Zhang¹ · Hongjian Guo²

Received: 19 July 2015 / Accepted: 11 November 2015 / Published online: 11 February 2016
© The Indian Institute of Metals - IIM 2016

Abstract In this work, Ni-based alloy coatings with different CeO₂ rare earth oxide contents were deposited on carbon steel by flame spray and fusing processing. The tribological behavior of the coatings was studied using a ball-on-flat wear tester under dry sliding, ambient conditions. Hardness testing, field emission gun scanning electron microscopy with attached energy dispersive spectroscopy and oscillating friction and wear testing were employed to characterize the microhardness, microstructure and tribological properties of the coatings. The results indicated that the addition of an appropriate amount of CeO₂ could refine and purify the microstructure. The coatings containing 5 wt% CeO₂ exhibited the highest wear-resistant properties. Moreover, a new compound phase, Ce₂Ni₂₁B₆, was formed within the coatings, such that the microhardness values containing this phase were higher than those in the other coatings. Finally, the effects of CeO₂ on the coatings and the mechanism describing the sliding wear were discussed.

Keywords Ni-based alloy · Cerium oxide · Flame sprayed · Tribology behaviour · Sliding wear

1 Introduction

Ni-based alloys have been widely used as coating materials for their ability to provide both wear and corrosion protection [1–3]. The most commonly employed Ni-based alloys are part of the Ni–B–Si system and contain other alloying elements. Nickel, being the major element, provides ductility and enhances the corrosion resistance [4, 5]. Coatings such as these are widely used in gas turbines and in the oil and steel industries, where sliding or erosion between one or more bodies is commonly encountered [6–8]. Nickel-based alloys may also be suitable for replacing cobalt-based alloys due to their excellent anti-wear properties [9, 10]. Rare earth metals, after appropriate refining and purifying, have been successfully used to modify material surface properties [11–17]. Compared to conventional thermal spraying, combined thermal spray and fusing processing results in higher adhesive bonding, less porosity and a more compact microstructure [8, 10]. The reported works on the tribological properties of thermal spray and fusing Ni-based alloys containing rare earth composite coatings have focused mainly on only abrasive wear characteristics. Therefore, friction and the wear mechanisms of the Ni-based alloy coatings with CeO₂ need to be systematically studied. In this work, Ni-based alloy coatings with different CeO₂ contents have been deposited on carbon steel using flame spray and fusing processes to investigate the tribological properties of Ni-based alloy coatings with CeO₂ under dry sliding conditions against SAE52100 steel at ambient conditions to explore the friction and wear mechanisms and to provide an experimental basis that will permit an expansion of the application of rare earth elements.

✉ Zhenyu Zhang
zhzhyu428@163.com

¹ Material Engineering Department, Lanzhou Institute of Technology, Lanzhou 730050, Gansu, China

² State Key Laboratory of Solid Lubrication, Lanzhou Institute of Chemical Physics, Chinese Academy of Sciences, Lanzhou 730050, China

2 Experimental Setup

The Ni-based alloy coatings containing 0, 1, 3, 5 and 7 wt% CeO₂ were deposited on 1045 carbon steel by using flame spray and fusing processing. The steel substrates were machined to dimensions of Ø26 mm × 10 mm. The substrate surfaces were rinsed with ethanol followed by acetone and blasted with sand (sieved through a size 40 mesh). The particles of the Ni-based alloy powders were 45–105 µm in size and spherical in shape. The nominal chemical composition of the powder was 0.6–0.8 C, 3.0–4.0 B, 4.0–5.0 Si, 14.0–16.0 Cr, ≤5.0 Fe, and balance Ni (wt%). Cerium dioxide was provided by the General Research Institute of Mining and Metallurgy that was in excess of 99 % pure. The CeO₂ particles were 20–55 µm in diameter. The Ni-based alloy powder and CeO₂ powder were mixed and put into a stirrer and stirred for 10 min before flame spraying.

The flame spraying was carried out with an oxy-acetylene SPH-2/h gun (China). Optimum processing parameters were: an oxygen pressure of 420 kPa, an acetylene pressure of 55 kPa, an acetylene flow rate of 0.95 m³/h and an oxygen flow rate of 1.3 m³/h. Flame remelting consisted of using an oxyacetylene flame to the coatings until the melting temperature (920 °C) was reached. It is a manual process, and the final quality of the coatings depends on the experience and ability of the operator. The final thickness of the coatings was approximately 0.8 mm.

The metallic phases in the coatings were analyzed by XRD using Cu Kα radiation. The XRD investigations were performed on an X'Pert PRO diffractometer. The microhardness measurements were performed on an MH-5-VM model microhardness tester with a 4.9 N load. Microstructural characterization of the coatings was performed using a field emission gun scanning electron microscope (FEGSEM) equipped with energy dispersive spectroscopy (EDS).

Dry sliding friction and wear testing without any lubricant were performed on an Optimol SRV oscillating friction and wear tester at a temperature of approximately 26 °C and a relative humidity of about 55 %. The ball material was SAE52100 steel with a hardness of HRC 62–63 and the diameter of the ball was 9.53 mm. The friction and wear testing were carried out at an oscillating amplitude of 1 mm, normal loads of 20–100 N, a frequency of 10–50 Hz (corresponding to a linear speed of 0.02–0.10 m/s) and for a duration of 20 min. The specimens were machined into discs with dimensions of Ø24 mm × 7 mm. Prior to the friction and wear testing, the disc surfaces were polished with 500-grit emery paper, the disc surface roughness ranged from 0.8 to 0.4 µm Ra, followed by cleaning in an acetone ultrasonic bath for 20 min and drying in hot air. The

wear volume loss was measured using a MicroXAM three dimensional surface profiler. The wear rates were calculated as $w = v/sf$, where v is the wear volume loss in mm³, s the total sliding distance in m and f is the applied load. The morphologies of the worn surface of the samples were examined using FEGSEM.

3 Results and Discussion

3.1 Microstructure and Phase Structure of the Coatings

Figure 1a, b show the FEGSEM micrographs. As shown in Fig. 1a, the commercial Ni-based alloy powder has a spherical morphology, which is typical of the atomization process employed for powder production [1]. The back

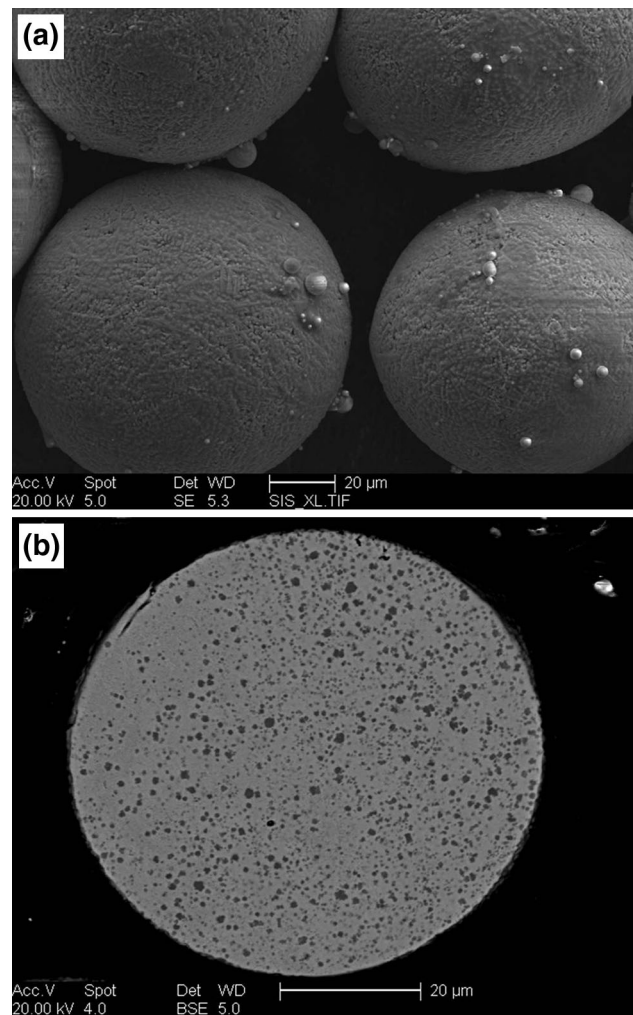


Fig. 1 Powder morphology of Ni-based alloy: **a** SEM image of the powders and **b** cross sectional BSE image of the powder

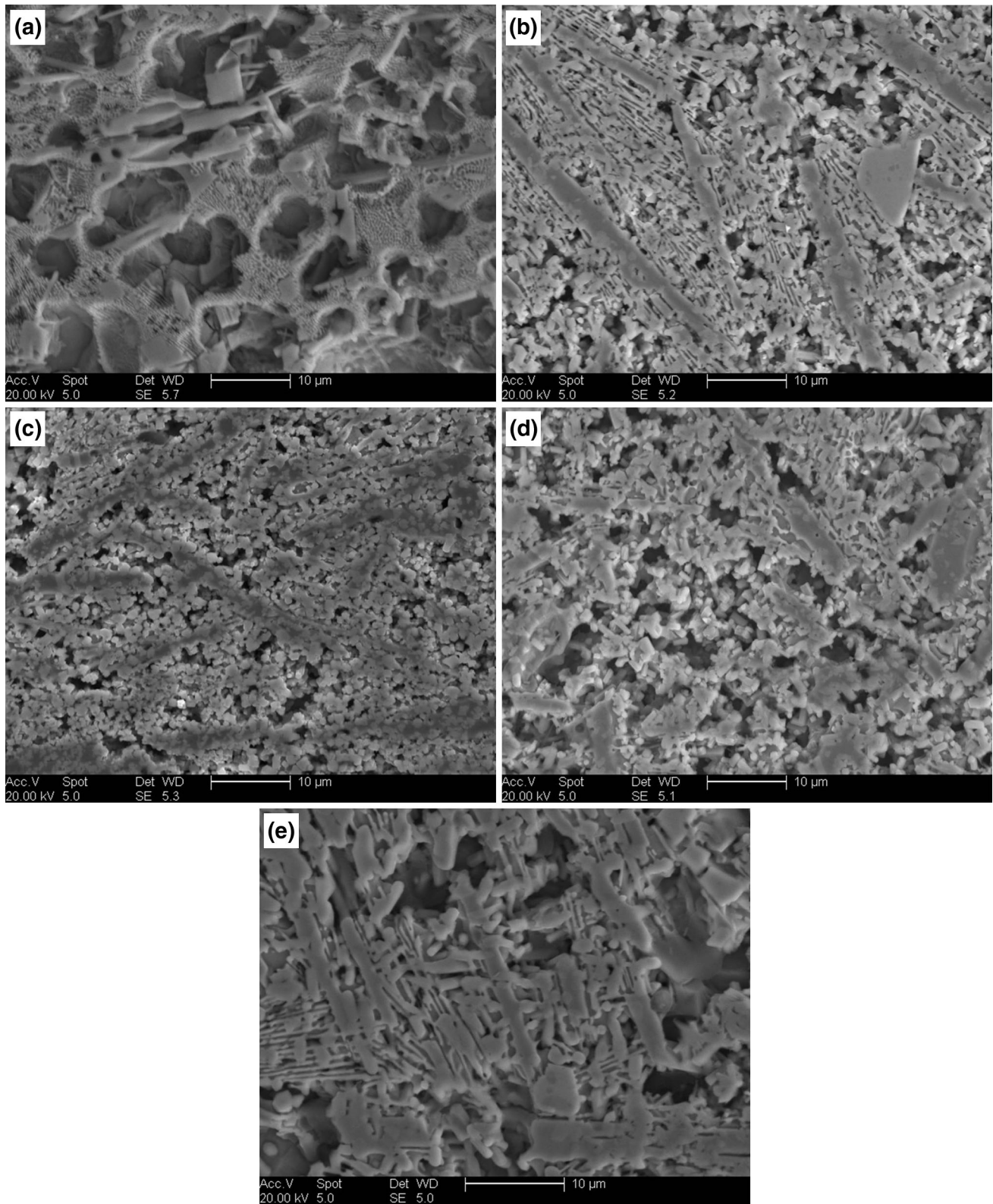


Fig. 2 Microstructure of the Ni-based alloy coatings with CeO₂: **a** 0 wt% CeO₂, **b** 1 wt% CeO₂, **c** 3 wt% CeO₂, **d** 5 wt% CeO₂ and **e** 7 wt% CeO₂

scattered image of a cross section of a powder particle is shown in Fig. 1b. The mean particle size is about 65 μm . The microstructure of the coating is shown in Fig. 2. The morphology of the coatings has been modified with the addition of CeO_2 . At the optimal CeO_2 content, the microstructure of the coating is finer than without CeO_2 , as shown in Fig. 2. However, it is noted that the addition of CeO_2 greater than a critical value, for example more than 5 wt%, results in poor quality coating, as shown in Fig. 2e. When the CeO_2 content is too low, the effects are similar to that seen for the 5 wt% CeO_2 content, as shown in Fig. 2b, c. The best CeO_2 concentration is 5 wt%, which yields the finest coating microstructure (in terms of the grain size). The results of the X-ray diffraction experiments are shown in Fig. 3. It shows the presence of $\gamma\text{-Ni}$, Cr_7C_3 , $\text{Ce}_2\text{Ni}_{21}\text{B}_6$, CrB and Ni_3Si in the coatings containing CeO_2 . A new compound phase, $\text{Ce}_2\text{Ni}_{21}\text{B}_6$, is identified in the coatings containing CeO_2 . However, the absence of peaks corresponding to CeO_2 may be attributed to the formation of the new phase. The presence of the $\text{Ce}_2\text{Ni}_{21}\text{B}_6$ results from the addition of CeO_2 . The amount of CeO_2 remaining after the formation of the new phase is too small to be detected. The

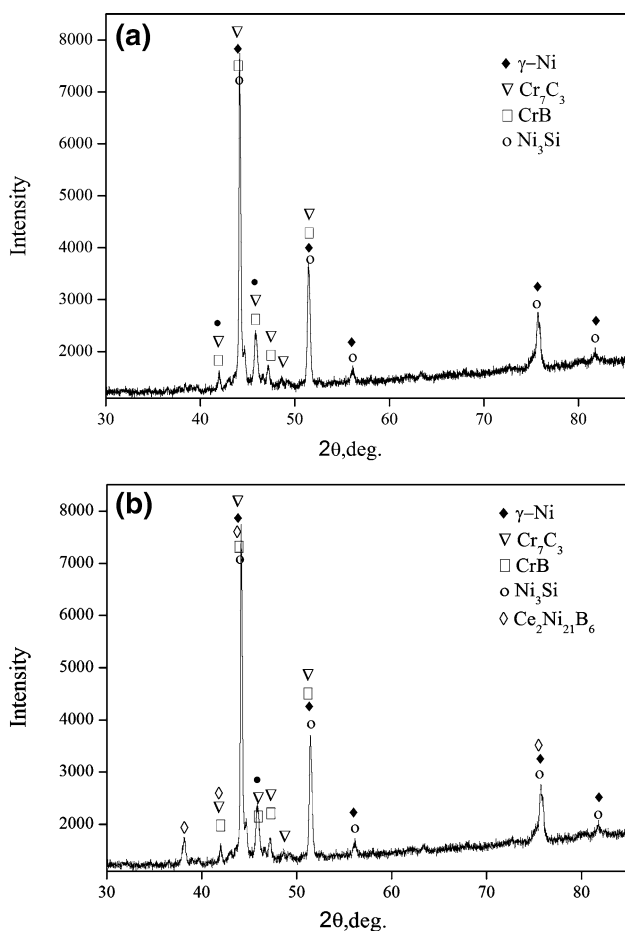


Fig. 3 XRD spectra of the Ni-based alloy coating: **a** 0 wt% CeO_2 and **b** 5 wt% CeO_2 coatings

addition of CeO_2 may result in a finer microstructure and yield a new compound phase within the coating. However, the absence of CeO_2 peaks in XRD spectra, has also been reported [13, 18]. It has also been observed that the high intensity of peak from the coatings correspond well to the formation of the new phase [19]. The back-scattered electron image of the coating containing 5 % CeO_2 and corresponding elemental distribution EDS map are shown in Fig. 4. The multiphase analysis systematically shows the presence of Ni, Cr, Si and Ce (Figs. 4b, 5, 6e), and reveals that Ni is abundant in region A (corresponding to the matrix phase of $\gamma\text{-Ni/Ni}_3\text{Si}$), Ni and Si are abundant in region B (corresponding to the eutectic phase of $\gamma\text{-Ni} + \text{Ni}_3\text{Si}$) and Cr is abundant in regions C and D (CrB , Cr_7C_3). Cerium is well distributed within the coating, as shown in Fig. 4e. A longitudinal section view of the Ni-based coatings containing CeO_2 and the elemental distribution are shown in Fig. 5, which consist of three distinct layers. From the top, these layers include a composite coating layer, an interfacial bonding zone and the substrate. Figure 5b, c show the X-ray elemental maps of Cr and Ni across the coating region. The coating area is rich with Cr and Ni, which are the main elements constituting the powder. It appears that the Ni and Cr diffuses in the interface, which indicate the presence of a metallic bond between the coating and the substrate.

It is well known that rare earth elements can refine the microstructure of alloys [9]. The refining effect of CeO_2 may be explained by the following. First, Ce is a surface active element with a rather large atomic radius (the radius of cerium is 0.1824 nm). The electronegativity of Ce is low (1.05 for Ce). This means that Ce can form positive ions and react easily with other elements, such as oxygen, sulfur, silicon and nitrogen. Therefore, some stable compounds, such as $\text{Ce}_2\text{Ni}_{21}\text{B}_6$ form during flame spraying and fusing processes. Cerium dioxide itself may form particles through heterogeneous nucleation. This can increase the number of crystal nuclei and hinder the growth of grains during crystallization of the molten pool [7]. However, during the course of crystallization, CeO_2 can act as a heterogeneous nucleation site for crystal nucleation and prevent grain growth during solidification. In addition, during the growth of nucleated grains, CeO_2 particles are pushed by the solid/liquid interface to the grain boundaries, as has been observed in metal matrix composites [7–9]. Third, Ce can reduce the surface tension and interfacial energy. Additionally, the chemical activity of Ce can also decrease critical nucleation work, causing the number of nucleation particles to increase. All of these factors result in a significant increase of the nucleation rate, meaning that the microstructure of the coating can be refined. Moreover, the chemical activity of Ce results in the formation of some high melting point compounds containing O, S and N

Fig. 4 Back scattered electron images of Ni-based alloy with CeO₂ and the Fe, Ni, Cr, Si and Ce elemental distributions

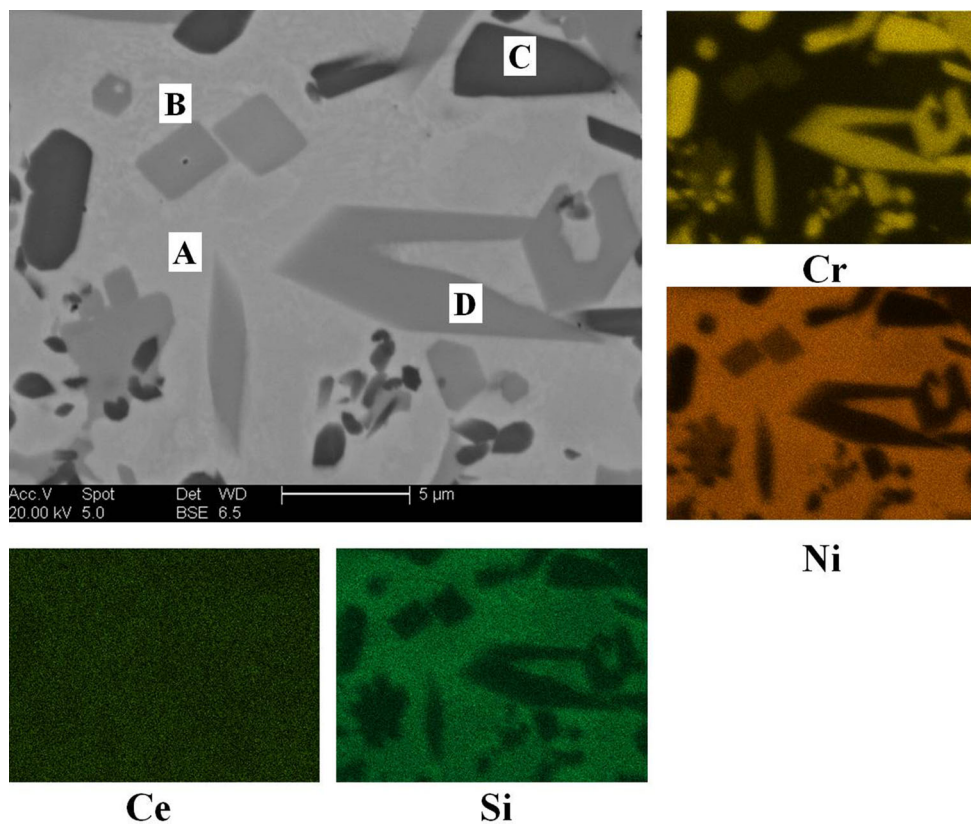
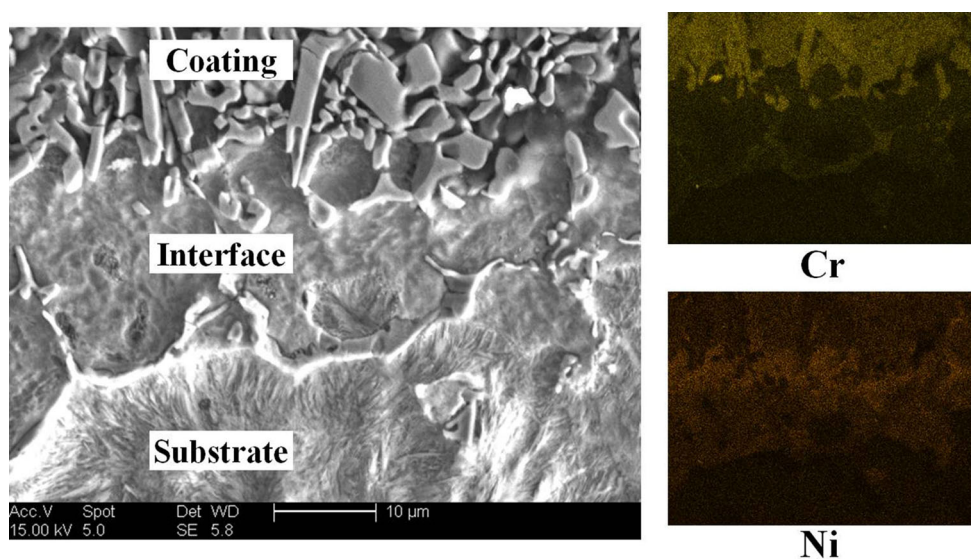


Fig. 5 Microstructure of the cross sectional morphology of the coatings containing CeO₂ and the Ni, Cr elemental distributions



during the cladding process. Portions of the compounds may float on the liquid phase prior to solidification and slag may occur on the surface of the sprayed coating [13]. Thus, the inclusion content within the coatings decreases, resulting in the purification of the coatings by deoxidation and desulfuration. As stated earlier, the addition of Ce can refine the grain size and purify the spray coatings. It should be emphasized that it is advisable to add only a certain

amount of Ce. Too much Ce is not beneficial to the microstructure and properties.

3.2 Hardness of the Coatings

Figure 6 shows the microhardness profile in the depth direction of the coating. The microhardness profile exhibits a graded distribution. On the surface of the coating, the

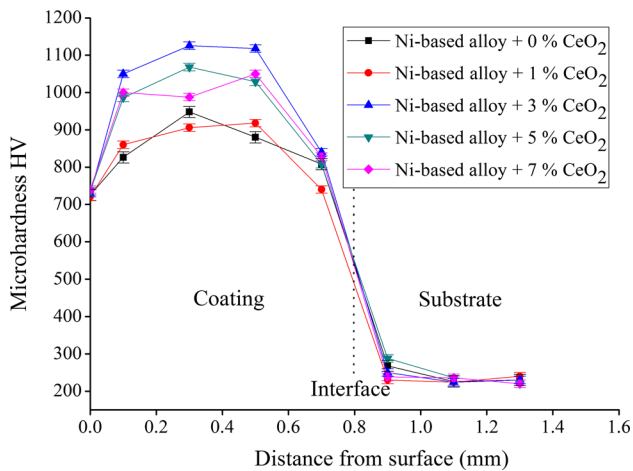


Fig. 6 Microhardness values on the sectioned surface for different coatings as a function of depth normal to the top surface

microhardness values are between 720 and 1120 HV. During the spraying process, the slag and impurities float from the molten pool. So the microhardness on the surface is relatively low. The data also shows that the addition of CeO_2 leads to varying microhardness values within the coatings. The hardness is highest when the 5 wt% Ce is added. An examination of the microstructure of the coating in Fig. 2 reveals that the microstructure of the coating containing 5 wt% CeO_2 is finer than the others, which implies that the hardness values also increase. Furthermore, when the CeO_2 addition is too high, the increased amount of entrapped slag material loosens the tissue and results in a decreased microhardness in the coating [20].

3.3 Friction and Wear Characteristic Under Sliding Tests

Variation in the wear rate of the Ni-based alloy coatings containing CeO_2 is shown in Fig. 7a. The sliding wear rate of the coatings containing approximately 5 wt% CeO_2 is lowest for all the specimens. However, excessive CeO_2 addition leads to only a small decrease in the wear resistance. This implies that Ni-based alloy coatings exhibit a higher wear resistance with the addition of 5 wt% CeO_2 . Variations in the coating friction coefficients under normal loading at a sliding speed of 0.05 m/s are given in Fig. 7b. The friction coefficient of the coatings containing 5 wt% CeO_2 decreases slightly and tends to be constant when under load. The SEM morphologies of the worn surfaces of the Ni-based alloy containing 5 wt% CeO_2 are shown in Fig. 8. Wear debris covers a portion of the worn surface. Additionally, there is a significant amount of material transfer. At a sliding speed of 0.04 m/s, the wear debris covers a portion of the worn surface. A large amount of

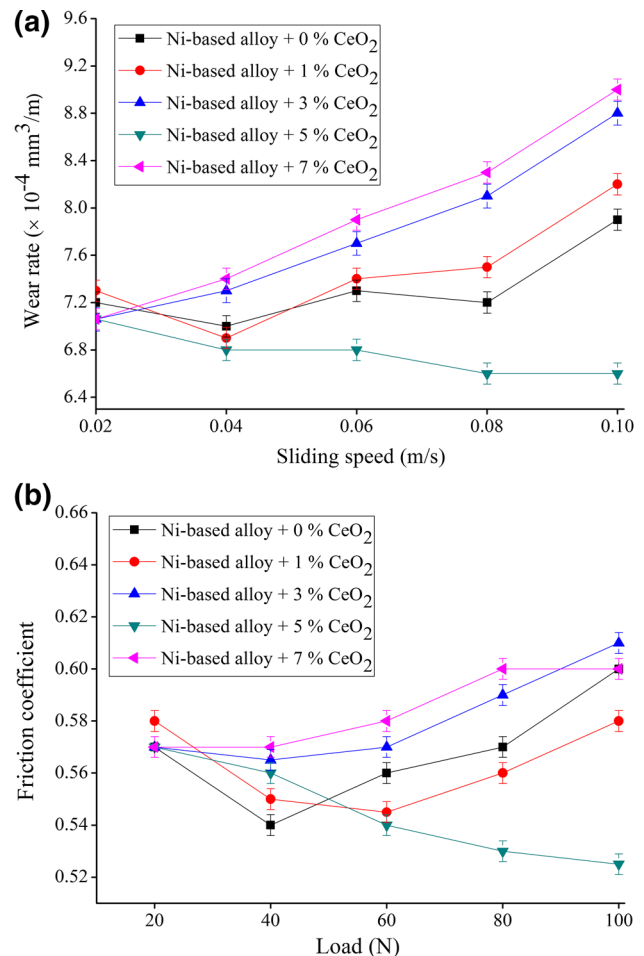


Fig. 7 Tribological properties of the coatings: **a** variation in the wear rate of the specimen at 40 N and **b** friction coefficient at a sliding speed of 0.05 m/s

wear debris covers the whole worn surface for the 0.1 m/s sliding speed. From these results, it is obvious that the wear debris layer becomes larger as the speed increases. Additionally, grooving is almost completely absent on the worn surface.

Figure 9 shows the SEM morphologies and elemental distributions of the adhesive transfer layer on the worn surfaces. Relatively large amounts of Fe and O exist on the adhesive transfer layer, and a relatively large amount of Ni and Cr are observed on the uncovered surface. The layer of debris on the worn surface is mainly transferred from the steel ball and oxidized during friction. In the opinion of the authors, the formation process can be explained as follows. The counterpart steel is a soft abrasive compared to the coating: it can neither press into, nor cut the coating effectively, but only slowly scratch the coating. At the same time, asperities within the coating possess a high hardness and can press and cut into the counterpart steel, which leads to the formation of an adhesive layer on the

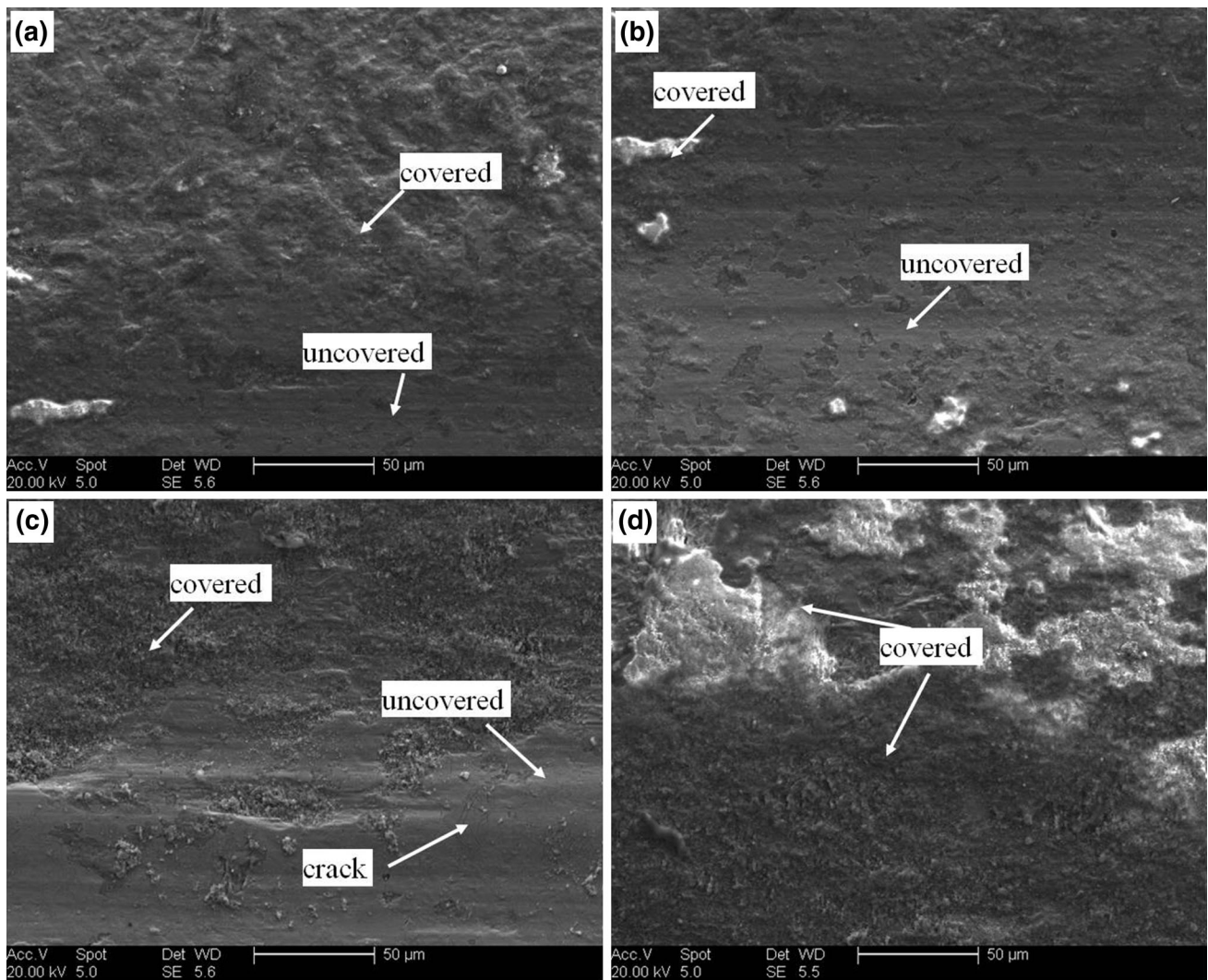


Fig. 8 FEGSEM morphologies of the worn surfaces of the Ni-based alloy coating containing 5 wt% CeO₂ after a sliding duration of 20 min at a linear speed of 0.05 m/s and normal loads of: **a** 40 N and **b** 80 N, at a normal load of 40 N and sliding speeds of **c** 0.04 m/s and **d** 0.1 m/s

wear surface. Therefore, the primary wear mechanism for the coatings is abrasive wear for normal loading and low sliding speeds, and adhesive wear for high loading and high sliding speeds. The wear resistance increases with the addition of the CeO₂, which can be attributed to the following. Cerium in the adhesive layer can reduce the wear and also have a self-lubricating effect; the lubrication function of CeO₂ at high temperatures has also been reported on [9, 13]. This accounts for the variation in the coating wear resistance with the addition of CeO₂. Furthermore, the refinement of the microstructure can increase the hardness of the coatings, and decrease instances of cracking and spalling in the reinforced phases during the wear process, which undoubtedly improves the adhesive and abrasive resisting abilities of the coating [9]. Finally, any excessive CeO₂ forms inclusions and reduces the microhardness. Therefore, there is no actual increase in the wear-resistance during metallic dry sliding wear processes

because of these contradictory factors [11]. In conclusion, there is an optimal amount of CeO₂. Too little or much CeO₂ is not beneficial to the microstructure characteristics and wear properties.

4 Conclusions

1. The microstructure of the coatings were refined and purified with an appropriate amount of CeO₂. The optimum addition of CeO₂ in this study was 5 %. A new phase, Ce₂Ni₂₁B₆, was formed in the coating containing 5 wt% CeO₂, and the existence of γ -Ni, Cr₇C₃, CrB and Ni₃Si was observed in coatings both with and without CeO₂.
2. The microhardness and wear resistance of the coatings with 5 wt% CeO₂ exhibited the best enhancement. Too

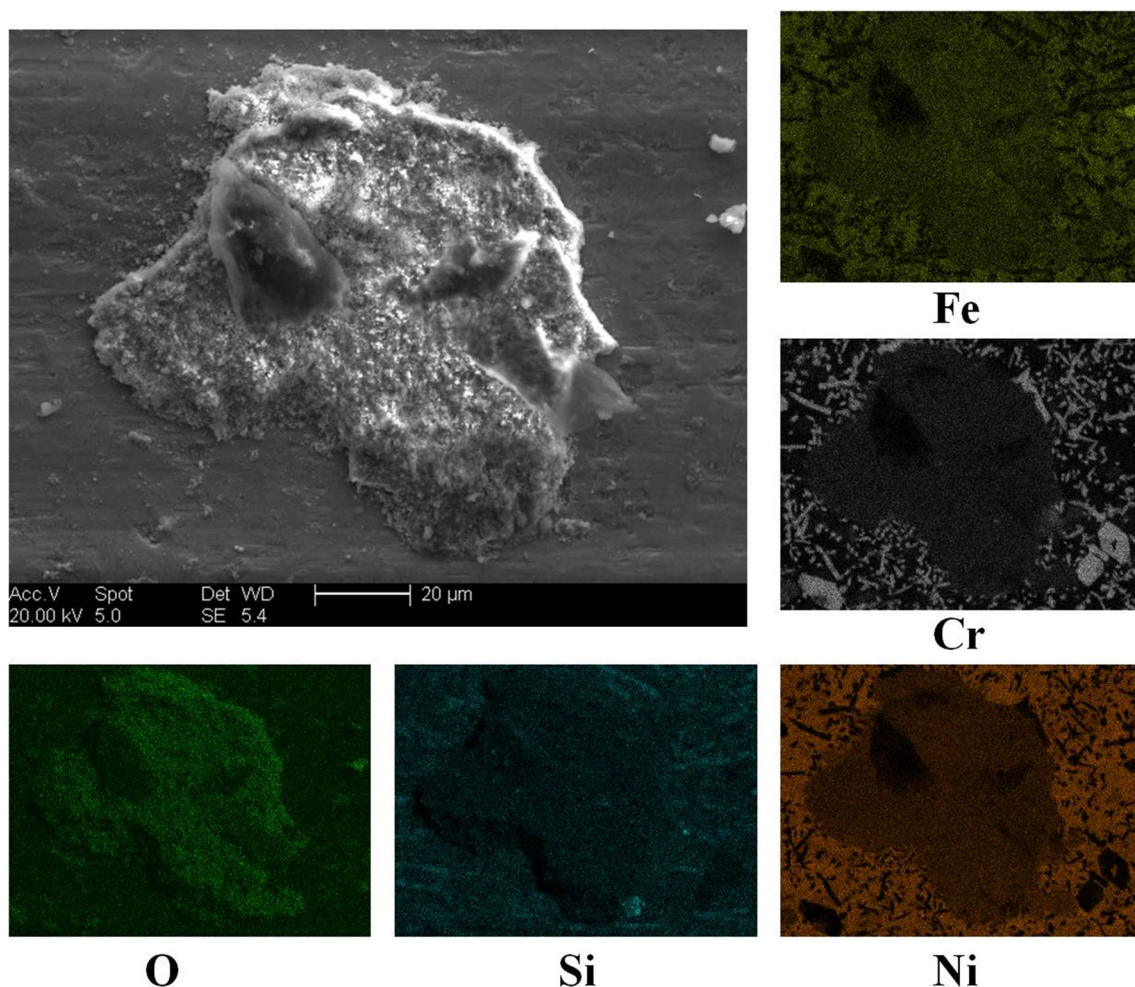


Fig. 9 FEGSEM morphologies and the Fe, Ni, Cr, Si and O elemental distributions of the adhesive transfer layer on the worn surface

little or too much CeO_2 was not beneficial to the microstructural characteristics and wear properties.

- The wear mechanism for the coatings was abrasive wear under normal loading and low sliding speeds, and adhesive wear under high loading and high sliding speeds.

Acknowledgments This study was financially supported by the National Natural Science Foundation of China (Nos. 51361020 and 51365024).

References

- Kim H-J, Hwang S-Y, Lee C-H, and Juvanon P, *Surf Coat Technol* **172** (2003) 262.
- Gonzalez R, Cadenas M, Fernandez R, Cortizo J L, and Rodriguez E, *Wear* **361** (2007) 153.
- Li Q, Song G M, Zhang Y Z, Lei T C, and Chen W Z, *Wear* **254** (2003) 222.
- Miguel J M, Guilemany J M, and Vizcaino S, *Tribol Int* **36** (2003) 181.
- Sharma S P, Dwivedi D K, and Jain P K, *Wear* **267** (2009) 853.
- Sunu R L, Yang D Z, Guo L X, and Dong S L, *Surf Coat Technol* **132** (2000) 251.
- Zhang Z Y, Wang Z P, Liang B N, Dong H B, and Hainsworth S V, *Wear* **262** (2007) 562.
- Zhang Z Y, Wang Z P, and Liang B N, *J Rare Earths* **23** (2005) 73.
- Zhang Z, Wang Z, and Liang B, *Tribol Int* **39** (2006) 1462.
- Zhang Z, Wang Z, and Liang B, *Tribol Int* **39** (2006) 971.
- Liang B, Zhang Z, Wang Z, and Chen B, *Rare Met* **29** (2010) 270.
- Zhang Z, Wang Z, and Liang B, *Rare Met* **27** (2008) 261.
- Zhang L, Sun D, and Yu H, *Mater Sci Eng A* **452–453** (2007) 619.
- Yu L G, Nie M D, and Lian Y F, *Wear* **197** (1996) 206.
- Wang K L, Zhang Q B, Sun M L, Wei X G, and Zhu Y M, *Corros Sci* **43** (2001) 255.
- Liu X-B, and Yu R-L, *Mater Chem Phys* **101** (2007) 448.
- Zhang Z Y, Lu X C, Han B L, and Luo J B, *Mater Sci Eng A* **454–455** (2007) 194.
- Wang K L, Zhu Y M, Zhang Q B, and Sun M L, *J Mater Process Technol* **63** (1997) 563.
- Yin B, Liu G, Zhou H, Chen J, and Yan F, *Tribol Lett* **37** (2010) 463.
- Lian Y, Yu L, and Xue Q, *Wear* **181–183** (1995) 436.